DOI: http://dx.doi.org/10.1590/2179-10742019v18i31628

Influence of Vegetation on the Outdoor-to-Indoor Mobile Radio Propagation in 700 MHz Band

Leonardo G. Ribeiro[1], Leni J. Matos[1], Pedro V. G. Castellanos[1], Matheus B. Moura[1], Vitor L. G. Mota[1], Wyliam D. T. Meza[2]
[1]*Fluminense Federal University, Niterói, Rio de Janeiro, Brazil*
leogr84@gmail.com, lenijm@id.uff.br, pcastellanos@id.uff.br, santozaw@hotmail.com, vitormota@id.uff.br
[2]*Universidad ALAS Peruanas, Lima, Peru*
w_torres_m@doc.uap.edu.pe

***Abstract*— Starting from outdoor transmission, crossing vegetation, the wideband and narrowband characterization of the indoor mobile radio channel in the 700 MHz band is obtained from experiments carried out in the indoor environment of the Engineering building at Fluminense Federal University, and from the processed data, respectively, the power-delay profiles obtained permitted to calculate the time dispersion parameters and the envelope of the signal permitted to adjust probability density functions to the signal variability, concluding about the influence of vegetation on those characteristics.**

***Index Terms*-** Channel characterization, channel statistics, delay spread, power delay profile, signal dispersion.

I. INTRODUCTION

The access to mobile networks has been growing notoriously throughout the world. The demand for this service was mainly due to the advance of the Internet access through mobile phones, smartphones, which made mobile network grow proportionally. The 4G (fourth generation) networks, in operation in many countries, have been gradually installed here in Brazil, and using LTE (Long Term Evolution) technology, it started on band 7, covering the 2600 MHz frequency. LTE was designed to support rates greater than 100 Mbps (downlink) and 50 Mbps (uplink) using a 2x2 MIMO scheme and 20 MHz bandwidth. This ensures optimal spectral efficiency and smaller connection latency time - less than 100 milliseconds. In addition, it has metrics such as resource requirements, priority in the routing queue, packet delay time, and packet loss rate to choose the best traffic route [1].

With the deactivation of open TV in Brazil, the 700 MHz band (named band 28) was released for cellular systems. Thus, the need for studies on this band for LTE is fundamental for a better understanding of the behavior of mobile radio channel in 4G technology, so that a wireless communication system can be correctly projected.

Several articles deal with this subject: Kaya and Calin [2] studied indoor coverage of the signal, using 3D ray tracing framework. There were also several features that have significant impact on the coverage and interference characteristics in a small cell environment, especially for multiple floors

Brazilian Microwave and Optoelectronics Society-SBMO *received 15 Feb 2019; for review 21 Feb 2019; accepted 10 June 2019*
Brazilian Society of Electromagnetism-SBMag *ISSN 2179-1074*

DOI: http://dx.doi.org/10.1590/2179-10742019v18i31628

buildings in urban environments in 700, 2100 and 2600 MHz. Measurements were performed and they also explored the delay spread behavior, concluding that RMS delay spread statistics are highly dependent on the environment. Wang *et al*. [3] investigated and compared the channel characteristics on two different floors in an outdoor-to-indoor communication. In [4] the channel characteristics were studied, but in 2.45 and 5.2 GHz frequencies. Among them: RMS (Root Mean Square) delay spread, power, NLoS (Non Line-of-Sight) error and coherence characteristics. However, vegetation was not present in the transmission link in these examples.

Moura *et. al* [5] applied artificial neural networks to narrowband data measured on a wireless indoor mobile communications scenario for 768 MHz outdoor transmission, in which the vegetation effect was embedded, confirming the advantage of using multilayer perceptron (MLP) neural networks for predicting coverage. With the same data of [5], Ribeiro *et. al* [6] analyzed the signal variability in this channel and besides this, with data obtained through wideband measurements in the same scenario and carrier, results for time dispersion parameters as average delay and RMS delay spread for the indoor channel in several floors with outdoor transmission are provided. Several articles deal with excess attenuation caused by a row of trees, at the level of trunks or canopies [7]- [8], forests [9]- [10], but the measurements occurred in outdoor environments, in general. In this context, the present work contributes with results of the experimental study of time dispersion and coverage statistics of an indoor reception signal coming from an outdoor transmission in the 768 MHz band, but with the focus on the influence of vegetation between the transmitter and the receiver on the coverage and the time dispersion of the signal. Vegetation is responsible for the absorption, shadowing, scattering, and depolarization of the signal and its presence plays an important role on the signal reception and its dispersion.

For that, this paper is structured as follows: Section II describes the transmission and reception system used in the sounding, besides the measurement environment; Section III deals with the channel characterization and the results; Section IV provides the conclusions for this work.

II. ENVIRONMENT AND SOUNDING SYSTEM SPECIFICATIONS

The environment chosen for performing the measurements was the Engineering School building of Fluminense Federal University in Niterói city, Rio de Janeiro, Brazil. Fig. 1 shows an aerial view of the outdoor environment where are highlighted the transmission point (TX), at 43 m height, and the Engineering School building, located at 40 m height and marked as RX, in red line, and pointing the sense of sounding along the five floors. The hall was also measured in that sense. Bold and dashed white lines show the distance of the initial and the final points to the transmitter, respectively, and they are 112 meters and 224 meters, respectively. It is noted that the signal crosses the vegetation between the transmitter and the receiver and it is important to confirm that the major part of the canopies are crossed by the link of TX to the third floor of the RX building. The vegetation is diverse with height of trees varying from 12 meters to 42 meters above the ground level. The lower trees are

  ISSN 2179-1074

DOI: http://dx.doi.org/10.1590/2179-10742019v18i31628

less dense and have more influence in the signal measured in the floors numbered as 1 and 2, while the taller trees are denser and their canopies are in the direction of the third floor of the measured building. Its extension along the direct ray (white line), in Fig. 1, was 108 m, and lateral vegetation extended along the whole Engineering School building.

On the day of the measurements, the weather was clear, without wind or rain. The transmission system (TX) was fixed, placed on the rooftop of Physics Institute building. The reception system was mounted in a mobile platform, moved at a speed of 1.2 m/s approximately, along the corridors of five floors and the hall located at the first floor of Engineering School building.

Fig. 1. Outdoor view of the measurement scenario.

A. Transmission Setup

Table I specifies the equipment and devices used in the signal transmission.

TABLE I. TRANSMISSION SETUP SPECIFICATIONS

Equipment/Device	Specification
Vector Signal Generator	Anritsu MG 3700A
Power Amplifier	Minicircuits ZHL-16W-43+
Digital Power Supply	ICEL PS-5000
Sectorial Antenna	RFS APX75-866512-CTO Beamwidth: 65 degrees Frequency: 698-896 MHz Gain: 14 dBi
Cable RG 213	Cable 1: 1 m, with 0.2 dB loss Cable 2: 2 m, with 0.5 dB loss

In the narrowband sounding, a 768 MHz carrier was the CW (continuous wave) signal transmitted to the channel. In the wideband transmission, a 20 MHz-bandwidth OFDM signal (previously generated in Matlab programming environment, transferred and saved in the memory of vector signal generator at the laboratory) was amplified and conducted to 14 dB-gain antenna in order to radiate in the same carrier.

At the generator output, the power level was -11 dBm so that the power saturation of the power amplifier (PA) did not occur. Its biasing was performed by the PS-5000 power supply. In Fig. 2 it is represented the block diagram of the transmission setup. Fig. 3 shows the setup mounted and the view of the transmitting antenna.

DOI: http://dx.doi.org/10.1590/2179-10742019v18i31628

The information signal transmitted was a pseudorandom (PN) sequence of 1023 bits with OFDM modulation. The choice for that sequence is on its characteristics of autocorrelation, which permits to identify easily the received OFDM symbols. The number of carriers was chosen equal to 2048 (1024 with sampling factor equal to 2) and the number of samples of the cyclic prefix was 128 (equivalent to 1/16 of the total number of carriers), as used in [11]. Then, these values were transformed into complex symbols and converted to time domain. The cyclic prefix was inserted and the real and imaginary components were separated to form the in-phase and quadrature components of the OFDM signal transferred to the vector signal generator.

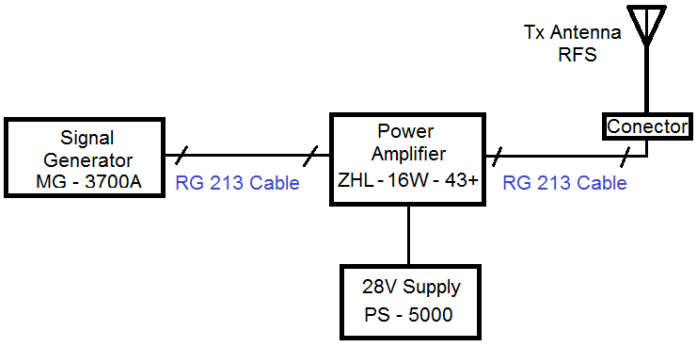

Fig. 2. Block diagram of the transmission setup.

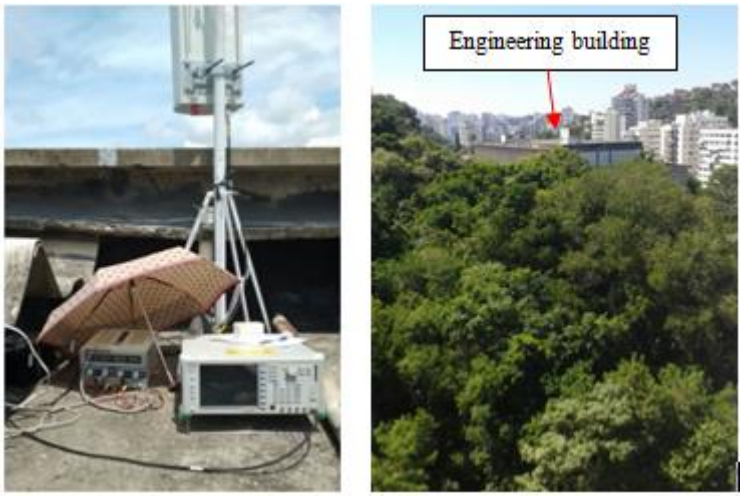

Fig. 3. Transmitter system: (a) setup; (b) view of the transmitting antenna.

B. Reception Setup

The block diagram of the reception (RX) setup is shown in Fig. 4. An omnidirectional antenna was installed on a mobile stand and a RG213 cable led the received signal to the input of a low noise amplifier (LNA), polarized by the 5 V source. The LNA was connected to the MS 2692A, which was used as a spectrum analyzer acquiring 123 samples/second (= 40 v/λ [5]) of the received CW for the narrowband sounding, and as a signal analyzer capturing "I" (in-phase) and "Q" (quadrature) samples of the OFDM signal, at a rate of 50M samples/s, for the wideband sounding. The data were transferred to the laptop via the network cable. To measure the location of the points, a GPS (Global Positioning System) device was connect to the laptop via USB (Universal Serial Bus) cable.

received 15 Feb 2019; for review 21 Feb 2019; accepted 10 June 2019

ISSN 2179-1074

DOI: http://dx.doi.org/10.1590/2179-10742019v18i31628

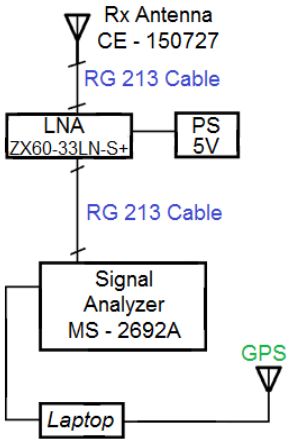

Fig. 4. Block diagram of the reception setup.

Table II provides the specifications of reception setup.

TABLE II. RECEPTION SETUP SPECIFICATIONS

Equipment/Device	Specification
Omnidirectional Antenna	CE-150727 Gain: 2 dBi for 768 MHz
GPS Device	GPS GarminMap 64S
Low Noise Amplifier (LNA)	Minicircuits ZX60-33LN-S+ Gain: 19.6 dB for 768 MHz
DC Power Supply MPL-1303 M	5 V
Vector Signal Analyzer	Anritsu MS 2692A
Laptop	*Dell Inspiron* 15
Cable RG 213	2 Cables: 1 m, with 0.2 dB loss

Fig. 5 shows a photo of the second floor of the measured building, indicating the sense of the receiver movement. The other floors are similar to it, only differing in number of chairs and/or benches and people. Measurements were performed along the corridors of the five floors and in the hall of the first floor, located beyond the door at the end of the measured corridor, and it is larger than the corridor as shows the layout in Fig. 6.

Fig. 5. Corridor on the second floor of the measured environment.

received 15 Feb 2019; for review 21 Feb 2019; accepted 10 June 2019

ISSN 2179-1074

DOI: http://dx.doi.org/10.1590/2179-10742019v18i31628

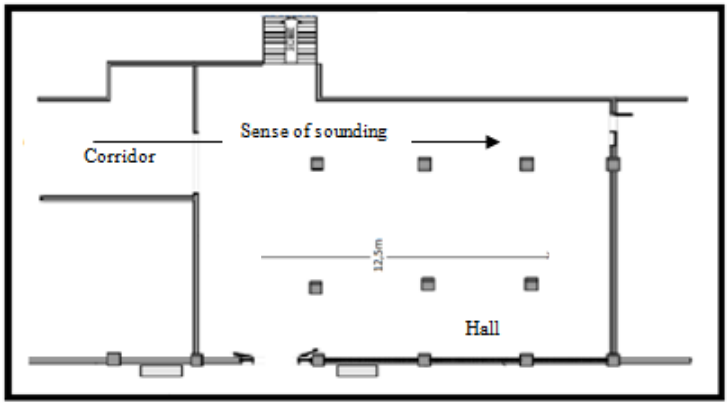

Fig. 6. Layout of the hall at the first floor of the measured environment.

III. CHANNEL CHARACTERIZATION RESULTS

A. Wideband Characterization

The randomness of the mobile radio channel makes stochastic the transfer function $h(t, \tau)$ defining the behavior of the propagation channel [12]. Based on [12]-[13] if the received signal passes through a filter matched to the transmitted signal (*s(t)*), the transfer function of the channel is the output of this filter. Therefore, the filtering process is equivalent to a correlation process (R_s), which will result in the instantaneous transfer function $h(t_i, \tau)$ of the channel:

$$h(t_i, \tau) = \sum_{i=1}^{N} C_i \, R_s(t - \tau_i, \tau) \tag{1}$$

in which τ stands for delay, C_i is the complex amplitude of the received signal (= *Re(s') + j Im(s')*) and *s'* is the quadrature signal measured at the reception by the vector signal analyzer. Then, the wideband characterization uses the received signal (I and Q samples) processed after a matching filter, i.e., $h(t_i, \tau)$, and provides the power delay profile (PDP), $P_h(t; \tau)$, calculated as proved in [12]. For this purpose, in each t_i, instantaneous power delay profiles are calculated from:

$$P_h(t_i, \tau) = |h(t_i, \tau)|^2 \tag{2}$$

For small times intervals or distances, the channel can be considered a WSSUS (Wide Sense Stationary Uncorrelated Scattering) channel [12] and its function can be expressed in four different domains as shows Fig. 7.

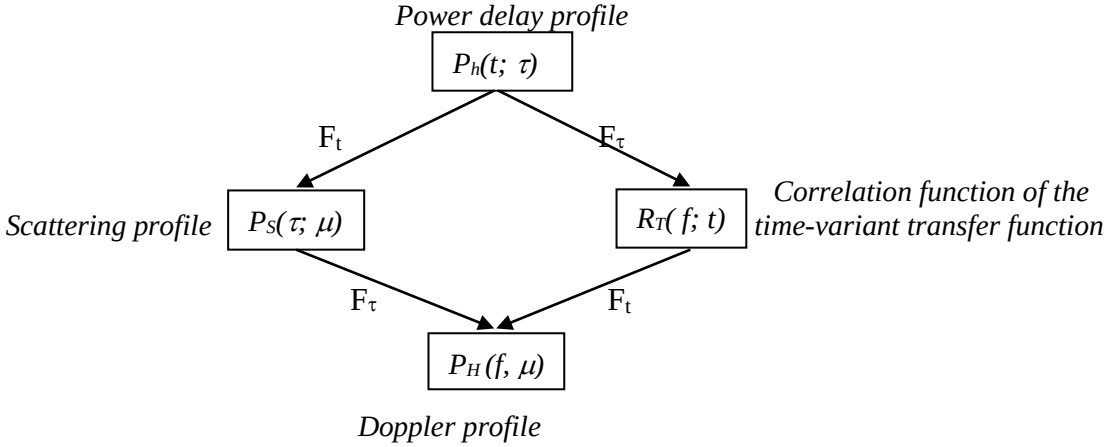

Fig. 7. Correlation function of WSSUS channels in all domains.

Brazilian Microwave and Optoelectronics Society-SBMO *received 15 Feb 2019; for review 21 Feb 2019; accepted 10 June 2019*
Brazilian Society of Electromagnetism-SBMag

ISSN 2179-1074

DOI: http://dx.doi.org/10.1590/2179-10742019v18i31628

The domains of the correlation functions are: time-delay ($t;\ \tau$), frequency-time ($f;\ t$), frequency-Doppler ($f;\ \mu$) and delay-Doppler ($\tau;\ \mu$), which can be obtained simply by DFFT (Discrete Fast Fourier Transform), and the calculated time dispersion parameters are the statistical moments of $P_h(t;\ \tau)$. Among them: the average delay (first central moment of P_h) and the delay spread (square root of the second central moment), known as RMS delay spread, calculated directly from PDPs samples [12].

The profiles calculated have the channel noise added to them. To mitigate the present noise and thus, to find the valid multipath in the PDPs, the CFAR (Constant False Alarm Rate) technique [14] was used. After its application, the time dispersion parameters were calculated for these cleaned PDPs and the results are in Table III. It is also provided the number of valid PDPs in each sounding and the mean of the delay spread values.

In general, RMS delay spread values are greater than that obtained in [2], whose mean value was 17 nanoseconds in 700 MHz for transmitter antenna with the same 14 dBi gain, but without vegetation between the transmitter and the receiver.

TABLE III. TIME DISPERSION PARAMETERS

Local	Mean delay (μs)	RMS Delay spread (D_s) (μs)	Mean D_s (ns)	No. PDPs
hall	0.11 - 6.11	0 - 6.52	782.2	22
1st floor	0.06 - 0.37	0 - 0.19	47.1	26
2nd floor	0.08 - 0.46	0 - 0.16	48.8	30
3rd floor	0.08 - 4.42	0 - 6.19	551.7	22
4th floor	0.17 - 0.41	0 - 0.19	111.2	26
5th floor	0.13 - 0.37	0.05 - 0.18	105.6	10

With the vegetation, that mean delay spread resulted in values from 47 to 782 microseconds, depending on the quantity of vegetation crossed by the signal. It is responsible by the scattering of the signal and, although it also absorbs part of its energy, it is a strong signal due to the 14 dBi gain of the transmitter antenna and the frequency used. Then, many paths of the signal arrive at the receiver, contributing for its time dispersion, including those scattered by the lateral vegetation. It is worth to observe that the number of walls also have influence in these results, but as it will be seen in the next item, Rice distribution will characterize the signal in all floors, indicating a strong ray reaching each floor.

Along the corridors, the results point the third-floor measurements strongly influenced by the vegetation due to the fact that the main beam of the directional antenna reaches the densest part of the vegetation, therefore, leading to higher RMS delay spread. In the hall, the dispersion was more pronounced, in general, due to the enlargement of this environment, contributing with more delayed multipath. Values of delay spread also are greater than that obtained in indoor-indoor transmission, generally of few nanoseconds, because there is the influence of the output scattering, mainly from the vegetation. This leads to smaller transmission rates for outdoor-to-indoor communication and techniques such as equalization and diversity guarantees greater rates.

received 15 Feb 2019; for review 21 Feb 2019; accepted 10 June 2019

ISSN 2179-1074

DOI: http://dx.doi.org/10.1590/2179-10742019v18i31628

B. Narrowband Characterization

The statistics of the signal small-scale variability was calculated in 40 λ-sectors in each corridor [15], totaling seven sectors in each floor. The acquisition rate of the CW signal envelope received was equal to 123 samples per second, corresponding to intervals of 0.025 λ (λ is the wavelength related to 768 MHz) between them, and sufficient to capture deep fading of the signal in indoor channel, said to be 0.05 λ in [15]. This interval will decay to 0.01 λ if the level of signal only results from multipath, in a NLOS environment [12].

The metric used for the error between the experimental (*f(x)*) and the theoretical (*g(x)*) probability density function (p.d.f.) of the small-scale signal is L^1, defined as [5]:

$$L^1 = \sum_{i=1}^{i=n} D(i) \tag{3}$$

with:

$$D = \int |f(x) - g(x)| dx \tag{4}$$

The smaller values of L^1 predominated for Rice p.d.f. (probability density function) for the sectors of the corridors, with K parameter varying between 6 and 36, leading to good fitting to Gauss p.d.f. too, although with a slightly greater error. Table IV presents the results for L^1 related to the second floor corridor, highlighting the smaller errors and confirming Rice p.d.f. as the best fitting with the K-factor varying between 8 and 20. Gauss p.d.f. is very close to it. The values for the other corridors presented similar characteristics.

TABLE IV. ERRORS FOR EXPERIMENTAL AND ADJUSTED P.D.F. IN THE SECTORS ON THE SECOND FLOOR

Sector/ p.d.f.	Gauss	Rayleigh	Rice	K- factor
1	**0.308**	0.908	**0.308**	14
2	0.409	0.993	**0.405**	14
3	0.187	0.767	**0.176**	8
4	0.233	0.986	**0.209**	18
5	0.298	1.020	**0.260**	20
6	**0.278**	1.012	0.281	18

Using a mobile average filter [16], the local mean of the level signal was calculated with a window of 320 samples and Fig. 8 shows some results for that mean. It is important to say that the measurements took 146.34 seconds per floor, except in the second one, in which they were performed in 154.47 seconds.

Summarizing, in applying the same filter to all floors and the hall, the p.d.f. related to the large scale signal resulted in the data of Table V. Rice p.d.f with high K-factor confirms the best adjustment, whose errors are highlighted and they are similar to the Gauss p.d.f. errors. Then, the mean behavior of the signal can be said gaussian.

received 15 Feb 2019; for review 21 Feb 2019; accepted 10 June 2019

ISSN 2179-1074

DOI: http://dx.doi.org/10.1590/2179-10742019v18i31628

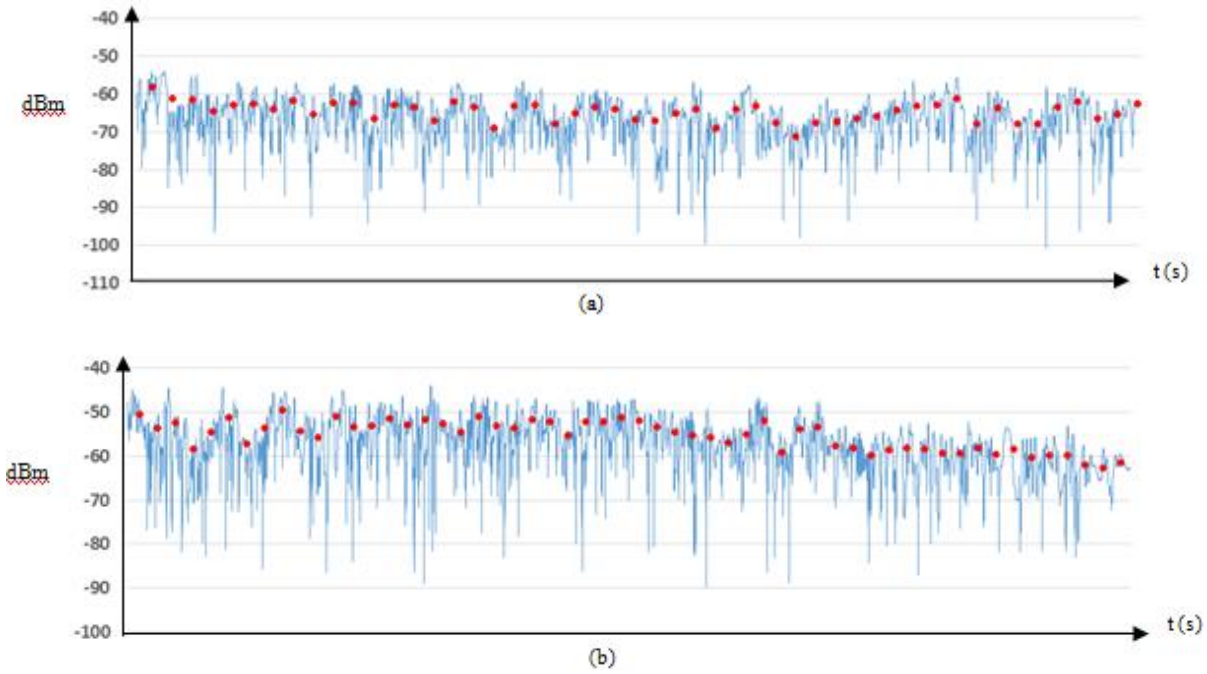

Fig. 8. Small-scale variability of the received signal (blue) and the local mean (red) along the corridors: (a) Third floor, and (b) Fifth floor

TABLE V. ERRORS EXPERIMENTAL AND ADJUSTED P.D.F FOR THE LARGE SCALE SIGNAL

p.d.f.	Gauss	Rayleigh	Rice	K- factor
2nd floor	0.799	2.595	**0.773**	26
3rd floor	0.916	2.648	**0.910**	21
4th floor	0.740	2.484	**0.726**	36
5th floor	0.844	2.683	**0.837**	24

Although the signal suffers attenuation due to the external environment between TX-RX, the vegetation and the building wall, its indoor behavior shows the confinement of the signal in the corridors, since it decays slowly along them as it is observed in Fig. 8. The smaller values of the signal occur in the third floor, in which the vegetation has more influence due to the absorption and scattering and they vary in the range of -57 to -70 dBm whereas they varied between -51 and -62 dBm in the fifth floor, which had sight to the transmitter, as shows Fig. 3(b). Therefore, in the third floor, the loss was increased by an average of 10 dB related to the fifth and the second floor. The Rice p.d.f. confirms the good level of the signal received in the TX-RX direction. This is observed in Fig. 9, where it can be seen that the signal also penetrates through the lateral windows besides crossing the walls. The smaller distance between TX-RX and the amount of vegetation crossed by the signal contribute for these results.

In Fig. 9, the hall position and the limits of the measured building are highlighted. The transmitting signal crosses the vegetation, but this is more intense for the path arriving in the third floor, leading to greater delay spread as it is noted in Table III.

received 15 Feb 2019; for review 21 Feb 2019; accepted 10 June 2019

ISSN 2179-1074

DOI: http://dx.doi.org/10.1590/2179-10742019v18i31628

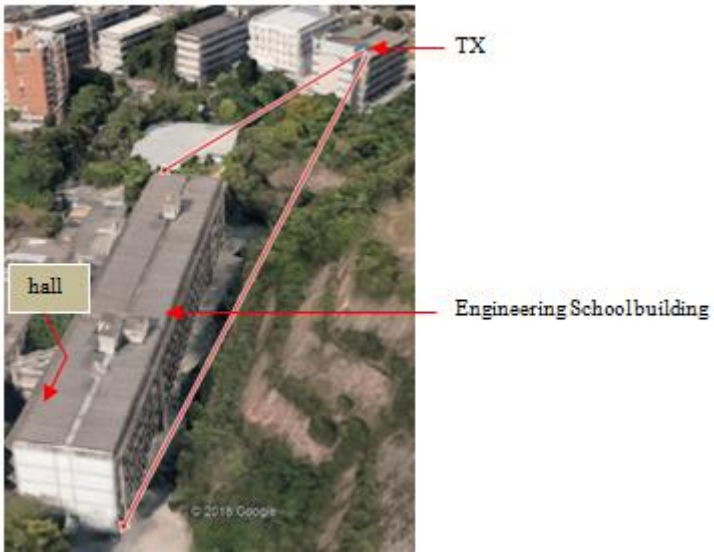

Fig. 9. Aerial view of the measured environment.

IV. CONCLUSION

The main goal of this paper was to characterize the indoor channel for the 700 MHz frequency band with outdoor transmission and vegetation between the transmitter and the receiver. Therefore, statistics of small and large scale fading, attenuation and time dispersion parameters were calculated and presented. For that purpose, the carrier of 768 MHz was used for narrowband sounding whereas an OFDM signal composed of 2048 carriers and in the range of 768 ± 10 MHz band was chosen for the wideband transmission. A directional antenna transmitted the signals from the top of a building and an omnidirectional antenna collected them in a reception module moving along the five floors and the hall of another building.

After processing, the calculated average delays and RMS delays varied in similar ranges in the first, second, fourth and fifth floors, presenting RMS delay spread values smaller than 190 nanoseconds and average values varying between 47.1 and 111.2 nanoseconds, in general. By observing the results, the fourth and fifth floors presented the RMS delay values near from the maximum values in the range (111.2 ns), whereas the first and second floors presented the nearest values from the minimum (47.1 ns). Relatively to the other floors, the greatest values occurred in the third floor, where average value was 551.7 nanoseconds for the RMS delay spread and the maximum of 4.42 microseconds for the mean delay. This is explained by the great number of multipath arriving at the receiver in the third floor coming from the canopy of the trees, which scattered the signal. It must be remembered that the propagation signal in 768 MHz band suffers less attenuation than signals in greater frequencies, therefore, good levels of signal arrive at the receiver. Then, more multipath coming from the trees can be detected, and this contributes with longer delays and, consequently, greater time dispersion. In the hall, the signal propagated in a wider area, with less confinement than the corridors, and different multipath are also generated in the walls, now with greater delays than in the corridors, leading to greater delay spread with mean equal to 782.2 nanoseconds.

DOI: http://dx.doi.org/10.1590/2179-10742019v18i31628

Comparisons with the mean value of 19 nanoseconds obtained for the experimental RMS delay spread values, calculated by Kaya [2] in similar distances, without vegetation between transmitter and receiver, show that vegetation has great influence in time dispersion. In the first, second, fourth and fifth floors these values reached from 2.5 to 6 times the Kaya value [2], while in the third floor, with more influence of the canopies of the trees, and in the hall, wider than the corridors, they are 29 to 41.1 times that value of 19 ns, respectively.

As the statistic of the small-scale signal variability, Rice was the best fitted p.d.f., confirming that there was a stronger ray coming through the wall and the windows located at the lateral of the building. For the large scale variability, Rice and Gauss p.d.f. provided similar fitting. Therefore, the signal presented Gaussian behavior in this indoor channel with outdoor transmission in the 700 MHz band and some dense vegetation between TX-RX.

Through this work, it was possible to understand the effect of vegetation on the behavior of the indoor signal at 700 MHz frequency band, originated from external transmission using a 14 dBi antenna. A mean loss of 10 dB over the signal amplitude was detected in the signal arriving at the floors when canopies of trees were crossed by the signal instead of their trunks and, mainly, the time dispersion of the signal reached average values of RMS delay in the range of 47.1-782.2 nanoseconds. Further measures will continue to be carried out in other environments in order to compare the vegetation effect on the received signal and, thus, to get complete indoor channel characterization when vegetation is present in the link TX-RX.

REFERENCES

[1] S. Sesia, I. Toufik, M. Baker; “LTE – The UMTS Long Term Evolution from Theory to Practice,” Chichester, West Sussex, 2011.

[2] A. O. Kaya, D. Calin; "On the Wireless Channel Characteristics of Outdoor-to-Indoor LTE Small Cells," *IEEE Transactions on Wireless Communications*, vol. 15, no. 8, pp.5453-5466, Aug. 2016.

[3] W. Wang, T. Jost, A. F. Dammann, and S. Kaiser, "Outdoor to indoor channel characteristics on two different floors," *European Transactions on Telecommunications*, vol.21, no. 5, pp.426-434, Aug. 2010.

[4] W. Wang, T. Jost, U-C. Fiebig, "A Comparison of Outdoor-to-Indoor Wideband Propagation at S-Band and C-Band for Ranging," *IEEE Transactions on Vehicular Technology*, vol. 64, no. 10, pp.4411-4421, Oct. 2015.

[5] M. B. Moura, D.C. Vidal, C. F. Schueler, L. J. Matos, T. N. Ferreira, “Outdoor-to-Indoor Power Prediction for 768 MHz Wireless Mobile Transmission using Multilayer Perceptron,” in *Int. Joint Conf. on Neural Networks* (IJCNN), 2018, pp. 1258-1264.

[6] L. G. Ribeiro, L. J. Matos, P. V. G. Castellanos, V. L. G. Mota, and W. D. T. Meza, "Experimental Characterization of Indoor Mobile Radio Channel in 700 MHz Band," in *IEEE MTT-S Latin America Microw. Conf.* (LAMC), Arequipa, Perú, 2018, pp 1-3.

[7] A. Tavakoli, K. Sarabandi, and F. T. Ulaby, "Horizontal Propagation through Periodic Vegetation Canopies," *IEEE Transactions on Antennas and Propagation*, vol. 39, no. 7, pp. 1014-1023, Jul 1991.

[8] N. C. Rogers et. al, "A Generic Model of 1-60 GHz Radio Propagation through Vegetation - Final Report," May 2002.

[9] R. K. Tewari, S. Swarup, M. N. Roy, "Radio Wave Propagation through Rain Forests of India," *IEEE Trans. on Antennas and Propagat*ion, vol. 38, no. 4, pp. 443-449,1990.

[10] T. Tamir, "On Radio-Wave Propagation in Forest Environments," *IEEE Trans. on Antennas and Propagation*, vol. 15, No. 6, pp. 806-817, 1967.

[11] L. H. Gonsioroski, L. da Silva Mello, C. R. Ron and L. J. Matos, "Characterization of a Mobile Urban Radio Channel with an Improved Multicarrier Sounding Technique," *Journal of Microwaves, Optoelectronics and Electromagnetic Applications- Special Issue : Wireless Communication*, vol. 14, pp. 158-167, Sep. 2015.

[12] J. D. Parsons, “The Mobile Radio Propagation Channel,” John Wiley & Sons, 2nd. Ed., 2000.

received 15 Feb 2019; for review 21 Feb 2019; accepted 10 June 2019

ISSN 2179-1074

[13] U. R. Villanueva, G. L. Siqueira, L. J. Matos, P. V. G. Castellanos, and L. H. G. Furtado, "Experimental Evaluation of the Mobile Radio Channel Capacity in the 2.48 GHz Band," *Journal of Microwaves, Optoelectronics and Electromagnetic Applications*, vol. 16, pp. 471-480, 2017.

[14] E. S. Sousa, V. M. Jovanović e C. Daigneault, "Delay Spread Measurements for the Digital Cellular Channel in Toronto," *IEEE Trans. on Vehicular Technology*, vol. 43, no 4, pp. 837-847, Nov. 1999.

[15] T. S. Rappaport, "Wireless Communications Principles and Practice," USA: Prentice Hall Professional Technical Reference, 1995, 641, chapter 4, pp. 139-196.

[16] J. G. Proakis, "Digital Communications," 4th. Ed., Mc Graw-Hill, 2000.

Brazilian Microwave and Optoelectronics Society-SBMO *received 15 Feb 2019; for review 21 Feb 2019; accepted 10 June 2019*
Brazilian Society of Electromagnetism-SBMag *ISSN 2179-1074*